

# Absolute-scale determination of bremsstrahlung following photoabsorption of incident x and $\gamma$ rays

---

Pašić, Selim; Ilakovac, Ksenofont

Source / Izvornik: **Physical Review A, 2000, 61, 42710 - 7**

Journal article, Published version

Rad u časopisu, Objavljena verzija rada (izdavačev PDF)

<https://doi.org/10.1103/PhysRevA.61.042710>

Permanent link / Trajna poveznica: <https://um.nsk.hr/um:nbn:hr:217:589747>

Rights / Prava: [In copyright](#) / [Zaštićeno autorskim pravom.](#)

Download date / Datum preuzimanja: **2025-01-15**



Repository / Repozitorij:

[Repository of the Faculty of Science - University of Zagreb](#)



## Absolute-scale determination of bremsstrahlung following photoabsorption of incident x and $\gamma$ rays

S. Pašić and K. Ilakovac

*Department of Physics, Faculty of Science, University of Zagreb, Bijenička cesta 32, HR-10000 Zagreb, Croatia*

(Received 7 October 1999; published 13 March 2000)

The spectrum of bremsstrahlung due to photoelectrons ejected by incident photons of energy 59.5 keV was measured on an absolute scale. A coincidence experimental setup with two high-purity germanium detectors was used. One detector served as the target as well as the detector of ejected electrons and another (second) detector served as the detector of bremsstrahlung radiation. The applied experimental method gives a very clean bremsstrahlung spectrum which can be reliably determined on an absolute scale in the low- and mid-energy range. Detailed processing of the data is presented, including calculations of all other processes that have also been recorded in the experiment. A simple theoretical model for the bremsstrahlung of photoelectrons in an infinitely thick target is applied and the results are compared with experimental values. Good agreement between the theoretical and experimental results has been obtained.

PACS number(s): 32.80.Cy, 32.30.Rj

### I. INTRODUCTION

Bremsstrahlung of low-energy electron beams has been extensively studied [1,2]. Energy spectra and angular distributions have been determined for a wide range of incident electron energies and for targets of various compositions and thickness.

Bremsstrahlung is also produced by low-energy ( $< 1$  MeV) photons (in the following we consider only that source of bremsstrahlung). It is due to electrons ejected by the photoelectric and Compton effects. In many experiments, the bremsstrahlung induced by incident photons contributes very little to the observed parts of the measured photon spectrum, and can be easily subtracted.

In some experiments the bremsstrahlung induced by incident photons is visible and more intensive at low energy than the investigated process(es). Examples are the spectra obtained in coincidence measurements of Compton scattering from  $K$ -shell electrons [3–5]. In some analyses of these spectra, the bremsstrahlung contribution is estimated by fitting the low-energy data with a function proportional to  $1/E_{ph}$  (where  $E_{ph}$  is the bremsstrahlung photon energy), which describes the bremsstrahlung contribution very well. The Compton-scattering data obtained show a low-energy tail and they are in agreement with results calculated using the impulse approximation [3,4]. The recent availability of  $S$ -matrix calculations by Surić *et al.* [6] and Bengstrom *et al.* [7] has allowed reanalyses of available Compton spectra and indirectly of the bremsstrahlung contribution in the Compton-scattering experiments. Based on their calculations, these authors found that in analysis of the data obtained in scattering of 59.54 keV photons from  $K$ -shell electrons in zirconium [4], a significant Compton contribution was subtracted together with the bremsstrahlung contribution. It should be noted that in the cases of a non-negligible amount of low-energy Compton-scattered photons, the fitting procedure cannot distinguish the low-energy Compton-scattered data and the bremsstrahlung data because of their very similar energy dependence. Therefore, accurate deter-

mination of the bremsstrahlung spectra on an absolute scale is recommended for analysis of the low-energy data obtained in Compton-scattering experiments.

It is very difficult to experimentally estimate or to considerably reduce the bremsstrahlung produced by photons incident on a target. Many measurements of Compton spectra were made using very thin targets with the aim of reducing bremsstrahlung to insignificant levels. In other measurements, targets of several thicknesses were used to deduce the bremsstrahlung contribution from the thickness dependence. These approaches were based on the naive assumption that electron multiple scattering could be neglected in thin targets. Recent studies show that even when the target thickness  $t$  is of the order of only 10% of the electron range  $R$  calculated in the continuous-slowing-down approximation, the bremsstrahlung intensity approaches its limiting values [8]. Also, even in the case of very thin targets, when  $t$  is 5% of  $R$ , the effect of electron multiple scattering is not negligible, causing a considerable presence of bremsstrahlung radiation [9–11].

A comprehensive theoretical treatment of the bremsstrahlung radiation induced by a beam of incident photons is a difficult problem. One has to take into account various effects like the angular distribution of photoelectrons, the energy loss and angular distribution in multiple elastic and inelastic scattering, the anisotropy of bremsstrahlung emission, the thickness of the target, etc. Such a detailed calculation of the bremsstrahlung process is accurate, but very tedious.

Another approach is the use of approximate models which considerably simplify the calculation. The thick-target approximation is of special interest, because it is encountered in many experiments. In a thick target, an electron experiences a large number of deflections, and some effects become irrelevant. For example, the angular distributions are averaged because the directions of electron velocity are randomized. Therefore, the complicated calculation of the bremsstrahlung spectrum can be considerably simplified with little loss of accuracy. One of the aims of the present work is the testing of such a simple model. The basis of the model was given in Ref. [12]. It was used in appropriate form in

Refs. [13] and [5] where it was extended to thick targets of arbitrary thickness.

In order to test the theoretical model, it is necessary to make an accurate measurement of the bremsstrahlung spectrum on an absolute scale. For this purpose we used an experimental setup with two germanium detectors and measured the bremsstrahlung produced by photoelectrons that were ejected from germanium atoms by incident 59.5 keV photons. The present experimental method is based on the coincidence detection of ejected electrons in the target detector and the bremsstrahlung photons in the second detector. Features of the experimental method and detailed processing of the data are presented, including calculations of all relevant processes. The same experimental arrangement, which we denote ‘‘asymmetrical setup’’ [14], was used in measurements of the Compton scattering by bound electrons in germanium [14–16]. We showed that this method gives very clean and reliable data on the Compton spectrum in a much wider energy range than that obtained in single-mode experiments [17,18].

To the authors’ knowledge, no bremsstrahlung spectrum following photoabsorption of incident photons has been published so far using the present experimental method. Ilakovac *et al.* [13] used a symmetrical variant of the coincidence setup for a bremsstrahlung measurement in which both Ge detectors were exposed to the photons from the source. Because of the very low number of counts, bremsstrahlung spectra were not observed and only the total counts were compared with the corresponding theoretical values. Corrections of the data for other nonbremsstrahlung processes (single Compton and reverse single Compton scattering), which contribute considerably, were not made. It should be noted that the symmetrical variant of the coincidence method is not a good choice for bremsstrahlung measurement and it cannot be applied for incident energy higher than about 30 keV because of the much stronger contribution of reverse Compton scattering.

## II. MEASUREMENT

### A. Experimental setup

A fast-slow coincidence system with a three-parameter ( $128 \times 512 \times 512$ )-channel pulse-height analyzer was used in the experiment. The system recorded a coincidence event if the time difference between the signals from the target and the second detector was less than 200 ns. Each event was represented as three numbers  $(k_0, k_1, k_2)$ , i.e., the time difference between pulses from the detectors, and the pulse-height from the target and from the second detector, respectively.

Two planar high-purity germanium detectors of nominal size  $200 \text{ mm}^2 \times 13 \text{ mm}$  thick were used in the measurement (see Fig. 1). The radioactivity of the source  $^{241}\text{Am}$  was about 39 kBq. The source was mounted on a source shield, which was placed between the detectors. The source shield was made of lead, with a cavity that was filled with  $\text{Dy}_2\text{O}_3$  and covered by a thin disk of Plexiglas. It served to expose essentially only the target detector to photons emitted from the source (asymmetrical setup). The asymmetry ratio  $A_s$ , i.e.,

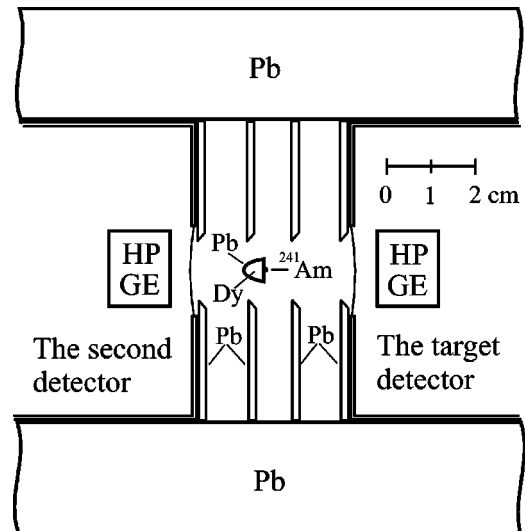


FIG. 1. Source, detectors, and shields of the experimental setup drawn to scale.

the ratio of numbers of 59.5 keV photons that reached the target detector and the second detector, was about 960. Four lead shields were placed between the detectors in order to define the scattering angle and to reduce photons that were elastically scattered into surrounding materials. The average scattering angle  $\vartheta_p$ , i.e., the angle between directions of the incident and the secondary photons that escaped the target detector and reached the second detector, was about  $170^\circ$ . The average solid angle  $\Delta\Omega_1$  of the second detector as seen from the collision points in the target detector was about 0.07 sr. The average solid angle  $\Delta\Omega_2$  of the target detector as seen from the collision points in the second detector had approximately the same value.

### B. Features of the experimental method and processing of data

Most photons of incident energy  $E_0 = 59.5 \text{ keV}$  that reach the active volume of the target detector are absorbed therein by the photoelectric effect. The energy absorption by Compton scattering is very small, and therefore bremsstrahlung of Compton electrons can be neglected. An ejected  $K$  or (seldom)  $L$  and  $M$  photoelectron loses its energy by radiating a bremsstrahlung photon [an emission of two photons per electron is relatively weaker by the factor  $(1/137)(\Delta\Omega/4\pi)$  and is neglected] or ionizing target electrons. The bremsstrahlung photons can escape the target detector and reach the second detector where they are absorbed. Coincidence detection of pulses due to the absorption of energy  $E_2$  of the bremsstrahlung photon in the second detector, and the absorption of the remaining energy  $E_1 = E_0 - E_2$  in the target detector is recorded as an event in the ‘‘events line’’  $E_1 + E_2 = E_0$ . Only data in the events line are taken into consideration in the processing of the bremsstrahlung data. Other events, which are, e.g., source-induced radiation of degraded energy prior to entering the active volume of the target detector or continuum due to the response function of the detectors, do not contribute to the observed events line.

The efficiency of the present method is very high because almost every ejected electron in the target detector is detected. On the other hand, the coincidence requirement essentially eliminates all exterior background. Therefore, a very high signal to background ratio is obtained. Both features allow measurements of a very long duration using sources of very weak activity (at least four to five orders of magnitude weaker than the sources used in other scattering measurements). Application of very weak sources almost entirely eliminates random coincidence events. The only events of that kind are peaks due to combinations of strong photon lines radiated from the source and of the characteristic x rays produced in the materials of the shields. These isolated peaks are widely spaced in the  $(E_1, E_2)$  two-dimensional spectrum and interfere very little with the narrow region of the events line  $E_1 + E_2 = E_0$  [full width at half maximum (FWHM)  $\sim 450$  eV].

The present experimental method allows the use of almost any radioactive source of x rays and  $\gamma$  rays, including cascades with crossover transition. Therefore, simultaneous measurements of the bremsstrahlung at several incident energies are possible in one experiment, namely, an events line  $E_1 + E_2 = E'_0$  due to incident photons of energy  $E'_0 < E_0$  cannot influence the data in the observed events line  $E_1 + E_2 = E_0$ . For  $E'_0 > E_0$ , the influence is very weak and corrections are needed only in the case of a much stronger line of a little higher energy than due to the observed events line.

It should be noted that the measurement of bremsstrahlung induced by photoabsorption of incident photons with a source-target-detector setup is not possible because the continuum of the detector response function from the Compton peak exceeds the bremsstrahlung spectrum by several orders of magnitude [17,18]. The source-target-detector setup would not allow measurement of the bremsstrahlung spectrum even if a system of detection that reduces the continuum of the detector response function [e.g., a detector with a NaI(Tl) anti-coincidence shield] were used.

#### Detector-to-detector scattering processes

The bremsstrahlung spectrum measured in the present experiment is one of the detector-to-detector cross-talk processes. Only these processes are observed in the present measurement. They are single cross-talk processes (single and reverse Compton scattering, escape of germanium  $K$  x rays) and double cross-talk processes. This list of the processes differs from the list of processes needing to be considered in processing of the data in a Compton experiment using the same coincidence setup [14]. Double scattering processes are not relevant for the bremsstrahlung experiment, but double cross-talk processes are included although they are not relevant in measurements of the Compton spectrum. These differences are the only ones in processing the bremsstrahlung data and Compton-scattering data obtained by the present experimental method. In Fig. 2 the results of calculations together with the unprocessed experimental spectrum obtained from the data in the events line  $E_1 + E_2 = E_0$  are shown as functions of energy absorbed in the second detector. Good agreement is obtained between the calculated and

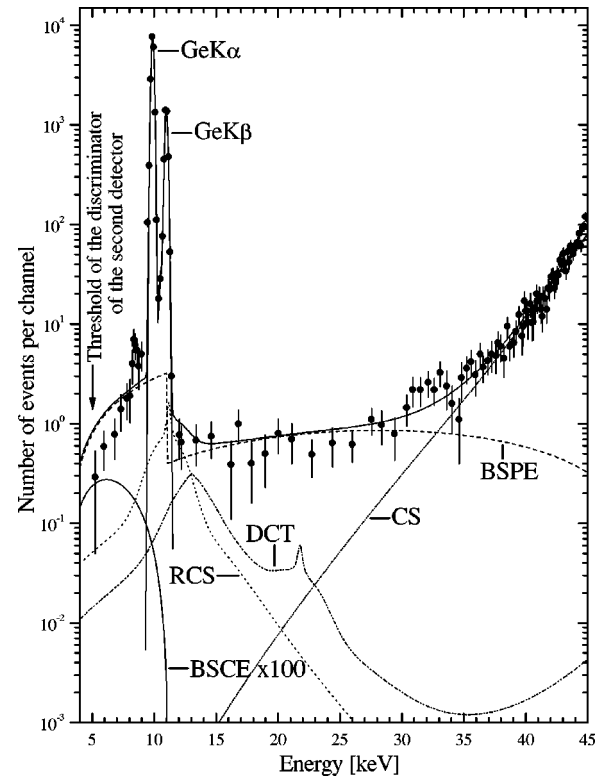


FIG. 2. Unprocessed experimental data in the events line  $E_1 + E_2 = E_0$  and calculated numbers of events of the processes shown as functions of energy absorbed in the second detector. BSPE, bremsstrahlung of ejected photoelectrons; CS, Compton scattering in the target detector; Ge  $K\alpha$  and Ge  $K\beta$ , cross-talk peaks due to characteristic  $K$  x rays of germanium; RCS, reverse Compton scattering; DCT, double cross-talk processes; BSCE, bremsstrahlung of ejected Compton-scattered electron (multiplied by 100).

experimental values. The calculation shows that bremsstrahlung of Compton electron is minor, as was expected. It is seen that the measured bremsstrahlung spectrum produced by photoelectrons is limited by the single Compton scattering at high energies and by the threshold of the discriminator of the second detector at low energies. Two large peaks due to cross talk between the two detectors via characteristic germanium  $K$  x rays are clearly seen. They are used to determine the absolute scale. The contribution of the reverse Compton scattering (due to events when primary photons pass the source shield, are Compton scattered in the second detector, and scattered photons enter the target detector and are absorbed therein) is weak because of the good asymmetry ratio of the experimental setup. A relatively weak contribution arises from a group of processes denoted as double cross talk between the two detectors. In these processes, photons of incident energy are scattered in the target detector, secondary photons escape it and reach the second detector where they are also scattered, and finally tertiary photons escape the second detector, reach the target detector, and are absorbed therein.

The number of events per channel due to single cross-talk scattering processes, in which energy  $E$  is deposited in the second detector, is calculated using the expression



$$n(E_0, E) = N_0 N_{\text{Ge}} \frac{d^2 \sigma(E_0, E, \vartheta_p)/d\Omega dE}{\mu(E_0) + \mu(E)/\cos \vartheta_p} \Delta D_1(E) A_2, \quad (1)$$

where

$$\Delta D_1(E) = \epsilon_c \epsilon_2 \epsilon(E) \exp[-\mu_{\text{air}}(E)d] \Delta \Omega_1.$$

$N_0 = 2.03 \times 10^8$  where  $N_0/\epsilon_1 \epsilon(E_0)$  is the number of photons of incident energy  $E_0 = 59.537$  keV that entered the target detector during the experiment,  $\epsilon_1 = \epsilon_2 = 0.95$  are the estimated efficiencies (not including the escape of characteristic Ge  $K$  x rays) of the target and second detector, and  $\epsilon(E)$  gives the efficiency of the target and the second detector involving only the escape of characteristic Ge  $K$  x rays.  $d^2 \sigma(E_0, E, \vartheta_p)/d\Omega dE$  is the differential cross section, and  $\mu(E_0)$  and  $\mu(E)$  are the attenuation coefficients in germanium [19,20] for the incident energy and energy  $E$  of the scattered photons.  $\epsilon_c = 0.98$  is the efficiency of the coincidence,  $N_{\text{Ge}}$  is the atomic density in germanium,  $A_2 = 0.12$  keV/channel is the channel width of the second detector,  $\mu_{\text{air}}$  is the attenuation coefficient in air, and  $d = 4.5 \times 10^{-2}$  m is the average path length of scattered photons in air.

The number of events per channel due to reverse Compton scattering is calculated using the equation

$$n(E_0, E_0 - E) = \frac{N_0}{A_s} N_{\text{Ge}} \frac{d^2 \sigma(E_0, E, \vartheta_p)/d\Omega dE}{\mu(E_0) + \mu(E)/\cos \vartheta_{\text{rev}}} \Delta D_2(E) A_2, \quad (2)$$

where

$$\Delta D_2(E) = \epsilon_c \epsilon_1 \epsilon(E) \exp[-\mu_{\text{air}}(E)d] \Delta \Omega_2.$$

$\vartheta_{\text{rev}} = 157^\circ$  is the average angle between the direction of photons incident into the second detector and the direction of scattered photons that escape the second detector and reach the target detector. Different values of  $\vartheta_p$  and  $\vartheta_{\text{rev}}$  show that some photons of incident energy  $E_0$  are elastically scattered by the surrounding shields before they hit the second detector.

The starting point in the calculations of double cross-talk processes is Eq. (1). In the calculations, we take into consideration combinations of single scattering processes (Compton scattering, bremsstrahlung, and the escape of the Ge characteristic x rays) in one detector with the same processes in the other detector. An exception is the combination of escapes of Ge  $K$  x rays from both detectors since they do not give a coincidence event. Combinations of elastic scattering in the target detector with other single scattering processes in the second detector are also included.

We consider the single scattering processes of incident photons  $E_0$  in the target detector in which  $n_2(E_1)dE_1$  secondary photons of energy  $E_1$  in the energy interval  $E_1$  to  $E_1 + dE_1$  are produced, escape it, and enter the second detector, where they are also singly scattered. The number of produced tertiary photons of energy  $E_2$  per unit energy interval that escape the second detector and reach the target detector, where they are absorbed, is

$$dn_1(E_2) = n_2(E_1)dE_1 N_{\text{Ge}} \sum_j \frac{d^2 \sigma_j(E_1, E_2, \vartheta_p)/d\Omega dE_2}{\mu(E_1) + \mu(E_2)/\cos \vartheta_p} \Delta D_2(E_2), \quad (3)$$

where

$$n_2(E_1) = N_0 N_{\text{Ge}} \frac{\sum_i d^2 \sigma_i(E_0, E_1, \vartheta_p)/d\Omega dE_1}{\mu(E_0) + \mu(E_1)/\cos \vartheta_p} \times \exp[-\mu_{\text{air}}(E_1)d] \Delta \Omega_1.$$

$\sigma_i$  and  $\sigma_j$  are the cross sections for bremsstrahlung or single Compton scattering by electrons in the subshells  $i$  and  $j$  in germanium atoms of the target and the second detector, respectively. The energy deposited in the target detector is  $E_{D1} = E_0 - E_1 + E_2$  while the energy deposited in the second detector is  $E_{D2} = E_1 - E_2$ .

Because the number of (coincident) events per channel  $N(E_{D2})$ , in which the deposited energy in the second detector is  $E_{D2}$ , is required, the substitution  $E_2 = E_1 - E_{D2}$  must be made as well as summation over all combinations of energies  $E_1$  and  $E_2$  that give the same value of  $E_{D2}$ . Therefore, the following transformation of Eq. (3) gives the required number of counts:

$$N(E_{D2}) = \int_{E_{D2}}^{E_0 - B_i} n_2(E_1)dE_1 N_{\text{Ge}} \sum_j \frac{d^2 \sigma_j(E_1, E_1 - E_{D2}, \vartheta_p)/d\Omega dE_1}{\mu(E_1) + \mu(E_1 - E_{D2})/\cos \vartheta_p} \times \Delta D_2(E_1 - E_{D2}) A_2. \quad (4)$$

Integration of Eq. (4) must be performed using the following conditions for the value of  $E_{D2}$ :  $E_{D2} > E_{\text{tr}2}$ ,  $E_{D2} \geq B_j$ , and  $E_{D2} < E_0 - E_{\text{tr}1}$ , where  $E_{\text{tr}1}$  and  $E_{\text{tr}2}$  are the energies corresponding to the discriminator thresholds of the target and second detector, respectively.  $B_j$  is the value of the binding energy in the subshell  $j$  of germanium atoms.

Equation (4) is directly applicable for the calculation of combinations of Compton scattering and bremsstrahlung radiation (continuous distributions) in both detectors. For continuous energy distributions of secondary photons in the target detector, which induce the escape of Ge  $K$  x rays in the second detector, Eq. (4) takes the form

$$N(E_{D2}) = n_2(E_{D2} + E_{K\alpha,\beta}) N_{\text{Ge}} \times \frac{d\sigma_{K\alpha,\beta}(E_{D2} + E_{K\alpha,\beta}, \vartheta_p)/d\Omega}{\mu(E_{D2} + E_{K\alpha,\beta}) + \mu(E_{K\alpha,\beta})/\cos \vartheta_p} \times \Delta D_2(E_{K\alpha,\beta}) A_2. \quad (5)$$

$E_{K\alpha,\beta}$  is the energy of Ge  $K\alpha$  and  $K\beta$  x rays, and  $\sigma_{K\alpha,\beta}(E, \vartheta_p)$  is the cross section for their production by photons of energy  $E$  that enter germanium at the angle  $\vartheta_p$  with respect to the normal of its surface. In the calculation of  $n_2(E_{D2} + E_{K\alpha,\beta})$ , the additional condition  $E_1 > B_1$  must be satisfied. The combination of the escape of Ge  $K$  x rays from the target detector that induced continuous distributions in the second detector is given by

$$N(E_{D2}) = N_2 N_{\text{Ge}} \times \frac{-d^2\sigma_j(E_{K\alpha,\beta}, E_{K\alpha,\beta} - E_{D2}, \vartheta_p)/d\Omega dE_{D2}}{\mu(E_{K\alpha,\beta}) + \mu(E_{K\alpha,\beta} - E_{D2})/\cos\vartheta_p} \times \Delta D_2(E_{K\alpha,\beta} - E_{D2}) A_2 \quad (6)$$

where

$$N_2 = N_0 N_{\text{Ge}} \frac{d\sigma_{K\alpha,\beta}(E_0, \vartheta_p)/d\Omega}{\mu(E_0) + \mu(E_{K\alpha,\beta})/\cos\vartheta_p} \times \exp[-\mu_{\text{air}}(E_{K\alpha,\beta})d] \Delta\Omega_1.$$

The condition  $E_{K\alpha,\beta} \geq E_{D2} \geq B_j$  must be satisfied.

Combinations of elastic scattering of incident photons in the active volume of the target detector and single scattering processes in the second detector are formally identical to reverse single (Compton) scattering. Therefore, they are also calculated using Eq. (2) where  $N_0/A_s$  is replaced by

$$N_{\text{elastic}} = N_0 N_{\text{Ge}} \frac{d\sigma_{\text{elastic}}(E_0, \vartheta_p)/d\Omega}{\mu(E_0) + \mu(E_0)/\cos\vartheta_p} \times \exp[-\mu_{\text{air}}(E_0)d] \Delta\Omega_1, \quad (7)$$

and  $\vartheta_{\text{rev}}$  by  $\vartheta_p$ . Values of the elastic differential cross sections are calculated using tabulated values for the modified relativistic form factor [21,22].

Emission of bremsstrahlung by photoelectrons inside thick targets is an essentially angle-independent process. That allows the use of a large solid angle in the measurement in order to increase the counting rate. On the other hand, one can see from the relation for double cross-talk processes that the relative intensity of double cross-talk processes with respect to the bremsstrahlung process is proportional to  $\Delta\Omega$ . Therefore, in bremsstrahlung measurements by the present experimental method, relatively good angular definition is required if one wants to reduce the rate of double cross-talk to bremsstrahlung.

### III. RESULTS AND THEORY

To obtain the bremsstrahlung data, the experimental spectrum (Fig. 2) was corrected for the calculated numbers of events due to nonbremsstrahlung single cross-talk processes using Eq. (1) and double cross-talk processes using Eqs. (4)–(7). The experimental results in terms of cross sections were obtained using the relation

$$\frac{d^2\sigma_{\text{exp}}(E_0, E)}{d\Omega dE} = \frac{n_{\text{exp}}[\mu(E_0) + \mu(E)/\cos\vartheta_p]}{N_0 \Delta D_1(E)}.$$

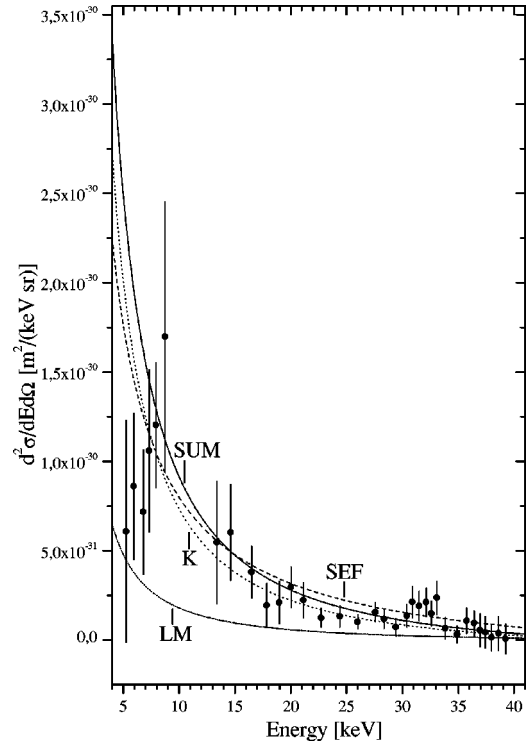


FIG. 3. The experimental and theoretical values of the differential cross section  $d^2\sigma/d\Omega dE$  for the bremsstrahlung of photoelectrons in an infinitely thick target.  $K$ , contribution of  $K$ -shell photoelectrons;  $LM$ , contribution of  $L$ - and  $M$ -shell photoelectrons;  $SUM$ , sum of  $K$  and  $LM$  contributions;  $SEF$ , contribution calculated by the semiempirical formula. The sharp decrease of the data at the low-energy end is due to the discriminator threshold of the second detector.

The result is shown in Fig. 3.

The model we used in the calculation of the bremsstrahlung radiation (see Fig. 2) is based on the fact that the mean path length of an electron of energy  $T_1$  in a thick target is related to its initial energy  $T_0$  [12] via the relation

$$\bar{s} = \int ds = \int_{T_1}^{T_0} \frac{dT}{dT/ds}, \quad (8)$$

where the energy loss of electrons per unit path length  $dT/ds$  is the sum of  $(dT/ds)_{\text{ion}}$  and  $(dT/ds)_{\text{rad}}$ , i.e., the energy losses per unit path length due to ionization and radiation, respectively. They are given by the approximate relations

$$\left(\frac{dT}{ds}\right)_{\text{ion}} = \frac{2\pi}{T} \left(\frac{e^2}{4\pi\epsilon_0}\right)^2 N_{\text{Ge}} Z \ln \frac{T\sqrt{2}}{I}$$

and

$$\left(\frac{dT}{ds}\right)_{\text{rad}} = \frac{16}{3} N_{\text{Ge}} Z^2 \sigma_0 (T + mc^2).$$

$I = (16 \text{ eV})Z$  ( $Z = 32$  for germanium) is the average ionization potential and  $\sigma_0 = (e^2/m_0c^2)^2/137 \text{ cm}^2/\text{nucleus}$ . The probability for production of a bremsstrahlung photon of en-

ergy  $E$  per unit energy interval and unit path length of an electron with energy  $T$  is given by

$$\frac{d^2W(T,E,s)}{dE ds} = N_{\text{Ge}} \frac{d\sigma_{\text{rad}}(T,E)}{dE}, \quad (9)$$

where  $d\sigma_{\text{rad}}(T,E)/dE$  is the cross section for bremsstrahlung radiation of an electron of energy  $T$  per unit energy interval of the radiated photon, which is given by the relation [12,23]

$$\frac{d\sigma_{\text{rad}}(T,E)}{dE} = BN_{\text{Ge}} Z^2 \sigma_0 \frac{T+mc^2}{TE},$$

where

$$B(x) = \frac{16}{3} \frac{1}{\sqrt{1-x}} \ln \left( \sqrt{\frac{1}{x}} - \sqrt{\frac{1}{x}-1} \right) \\ \times \frac{1 - \exp(-a/\sqrt{T})}{1 - \exp[-a/\sqrt{T(1-x)}]} \frac{mc^2}{mc^2 + T},$$

$x = E/T$ , and constant  $a = 2\pi Z\alpha \sqrt{mc^2/2}$ . Using Eqs. (8) and (9), one obtains the probability for production of a bremsstrahlung photon of energy  $E$  per unit energy interval by an electron ejected with initial energy  $T_0$ :

$$\frac{dW(T_0,E)}{dE} = \int_{E}^{T_0} \frac{d\sigma_{\text{rad}}(T,E)/dE}{(dT/ds)_{\text{rad}} + (dT/ds)_{\text{ion}}} dT. \quad (10)$$

That relation gives the differential cross section per atom for bremsstrahlung of ejected electrons,

$$\frac{d^2\sigma_{\text{BS}}(E_0,E)}{dE d\Omega} \\ = \frac{1}{4\pi} \sum_{i=K,L,M} \int_E^{T_{\text{max}}^i} \frac{d\sigma_i(E_0,T_0)}{dT_0} \frac{dW(T_0,E)}{dE} dT_0, \quad (11)$$

where  $T_{\text{max}}^i$  is the maximum energy of ejected electrons from shell  $i$ .  $d\sigma_i(E_0,T_0)/dE$  is the cross section for ejection of electrons from shell  $i$  with energy  $T_0$  per unit energy and per incident photon of energy  $E_0$ . In the case of photoabsorption, it is given by

$$\frac{d\sigma_i(E_0,T_0)}{dT_0} = \sigma_i^{\text{ph}}(E_0) \delta(T_0 - E_0 + B_i),$$

where  $\sigma_i^{\text{ph}}(E_0)$  is the cross section for photoabsorption of incident photons of energy  $E_0$  in the shell  $i$  of germanium atoms. In the case of Compton scattering, when we consider electrons as free and stationary, the cross section for electrons is given by [12]

$$\frac{d\sigma_i(E_0,T_0)}{dT_0} = K_i \frac{d\sigma_{\text{KN}}(E_0,E,\vartheta)}{d\Omega} \frac{2\pi}{\alpha^2 m_0 c^2} \\ \times \left[ \frac{(1+\alpha)^2 - \alpha^2 \cos^2 \varphi}{(1+\alpha)^2 - \alpha(2+\alpha) \cos^2 \varphi} \right]^2,$$

where  $K_i$  is the number of electrons in the shell  $i$  of the germanium atom,  $d\sigma_{\text{KN}}(E_0,E,\vartheta)/d\Omega$  is the well known Klein-Nishina formula for Compton scattering of unpolarized photons,  $m_0 c^2 = 511$  keV,  $\alpha = E_0/m_0 c^2$ ,  $\varphi$  is the scattering angle of ejected electrons, and  $\vartheta$  is the scattering angle of photons.

The relations used for the bremsstrahlung radiation cross section have been obtained in the Born approximation, and their accuracy decreases as electron energy decreases. The relation for energy loss due to ionization  $(dT/ds)_{\text{ion}}$  is also better at higher electron energies, i.e., when  $T \gg I$ . Both approximations make Eqs. (10) and (11) valid for energies of bremsstrahlung photons higher than approximately 1.5 keV (in germanium). From Eqs. (8) and (10) one can see that high-energy bremsstrahlung photons can be emitted only at the beginning of the electron path. That means that for high energies of the bremsstrahlung spectrum, Eqs. (10) and (11) are valid even when the target thickness is comparable to or smaller than the electron range, i.e., when neither the thin nor thick-target approximation is valid. The theoretical values derived from Eq. (11) are shown in Fig. 3 for  $K$  and  $LM$  photoelectrons, and their sum.

For comparison, the bremsstrahlung cross section of photoelectrons based on a well known semiempirical thick-target formula is also shown (Fig. 3). The formula is given by [24]

$$\frac{d\sigma_{\text{BS}}^{\text{SEF}}(E_0,E)}{dE d\Omega} = \frac{2kZ}{4\pi} \sum_{i=K,L,M} \sigma_i^{\text{ph}} \frac{E_0 - B_i - E}{E}. \quad (12)$$

In the literature, different values of the parameter  $k$  are used, reflecting the approximate nature of the semiempirical formula. We used  $k = 1.38 \times 10^{-6}$  keV $^{-1}$  as in Ref. [5], which is suitable for infinitely thick targets.

Agreement between the theoretical and experimental results is good.

#### IV. CONCLUSIONS

The present experimental method for measurement of the bremsstrahlung following absorption of incident photons shows several distinct features. Almost any line source of photons can be used even if of a complex spectrum. Thus, simultaneous measurements at several incident energies are possible in one experiment. Exterior background and source-induced radiation are eliminated, resulting in a very high signal to background ratio. The efficiency of the presented method is high since every ejected electron is detected. For comparison, the coincidence method for detection of bremsstrahlung due to  $K$  photoelectrons [3–5] would give at least a 10 to 20 times smaller counting rate under similar experimental conditions. Therefore, application of very weak sources is possible. The most important feature is that most

of the obtained bremsstrahlung data need very little correction, which makes final results very reliable on an absolute scale. That is, only a narrow high-energy region of the bremsstrahlung spectrum obtained is corrected for Compton scattering, and only a few points are not included because of the detection of two large peaks due to characteristic Ge  $K\alpha$  and  $K\beta$  x rays. Contributions of other processes are minor if the asymmetry ratio is higher than approximately 1000 (to reduce reverse Compton scattering), and the solid angle is

smaller than about 0.15 sr (to reduce the influence of double cross-talk processes).

The simple theoretical model of bremsstrahlung radiation due to photoelectrons in an infinitely thick target gives results in good agreement with the experimental data. Marchetti and Franck [5] extended it to targets of arbitrary thickness, but to our knowledge the improved model has not been rigorously tested so far. It could be very useful for a simple absolute-scale determination of bremsstrahlung, which is needed in processing low-energy Compton-scattering data.

- 
- [1] M. A. Short and E. J. Bonner, *X-Ray Spectrom.* **18**, 183 (1989).
- [2] S. Habib, M. J. Minski, and T. D. MacMahon, *Nucl. Instrum. Methods* **180**, 147 (1981).
- [3] J. Laukkanen, K. Hämäläinen, and S. Manninen, *J. Phys.: Condens. Matter* **8**, 2153 (1996).
- [4] S. Manninen, K. Hämäläinen, and J. Graeffe, *Phys. Rev. B* **41**, 1224 (1990).
- [5] V. Marchetti and C. Franck, *Phys. Rev. A* **39**, 647 (1989).
- [6] T. Surić, P. M. Bergstrom, Jr., K. Pisk, and R. H. Pratt, *Phys. Rev. Lett.* **67**, 189 (1991).
- [7] P. M. Bergstrom, Jr., T. Surić, K. Pisk, and R. H. Pratt, *Phys. Rev. A* **48**, 1134 (1993).
- [8] P. P. Kane, *Phys. Rep.* **218**, 67 (1992).
- [9] J. P. Briand, A. Simionovici, P. Chevallier, and P. Indelicato, *Phys. Rev. Lett.* **62**, 2092 (1989).
- [10] A. Simionovici, J. P. Briand, P. Indelicato, and P. Chevallier, *Phys. Rev. A* **41**, 3707 (1990).
- [11] V. Marchetti and C. Franck, *Phys. Rev. Lett.* **65**, 268 (1990).
- [12] R. D. Evans, *The Atomic Nucleus* (McGraw-Hill, New York, 1955).
- [13] K. Ilakovac, J. Tudorić-Ghemo, V. Horvat, N. Ilakovac, S. Kaučić, and M. Vesković, *Nucl. Instrum. Methods Phys. Res. A* **245**, 467 (1986).
- [14] S. Pašić and K. Ilakovac, *Phys. Rev. A* **55**, 4248 (1997).
- [15] S. Pašić and K. Ilakovac, *Fiz. B* **4**, 127 (1995).
- [16] S. Pašić, Ph.D. thesis, University of Zagreb, 1997 (unpublished).
- [17] P. Rullhusen and M. Schumacher, *J. Phys. B* **9**, 2435 (1976).
- [18] M. Schumacher, *Z. Phys.* **242**, 444 (1971).
- [19] D. E. Cullen *et al.*, Lawrence Livermore National Laboratory Report No. UCRL-ID-103424, 1990 (unpublished); Lawrence Livermore National Laboratory Report No. UCRL-50400, 1989 (unpublished).
- [20] J. H. Hubbell and S. M. Seltzer, National Institute of Standards and Technology, Report No. NISTIR 5632, 1995 (unpublished).
- [21] D. Schaupp, M. Schumacher, F. Smend, P. Rullhusen, and J. H. Hubbell, *J. Phys. Chem. Ref. Data* **12**, 467 (1983).
- [22] J. H. Hubbell, Wm. J. Veigele, E. A. Briggs, R. T. Brown, D. T. Cromer, and R. J. Howerton, *J. Phys. Chem. Ref. Data* **4**, 471 (1975).
- [23] W. Heitler, *Quantum Theory of Radiation*, 3rd ed. (Oxford University Press, London, 1954).
- [24] H. A. Kramers, *Philos. Mag.* **46**, 836 (1923).